

# Gel–gel adhesion by tethered polymers

Yanbin Huang

*School of Chemical Engineering, Purdue University, West Lafayette, Indiana 47907*

Igal Szleifer<sup>a)</sup>

*Department of Chemistry, Purdue University, West Lafayette, Indiana 47907*

Nikolaos A. Peppas<sup>a)</sup>

*School of Chemical Engineering, Purdue University, West Lafayette, Indiana 47907*

(Received 29 August 2000; accepted 11 December 2000)

The behavior of tethered polymers on gel/gel adhesion is studied with the single-chain mean-field (SCMF) theory. It is shown that the gel surface structure, the gel/gel adhesion strength, the equilibrium gel/gel distance, and the detailed interface structures can be tailored by specifically designed tethered layers on gel surfaces. The SCMF theory allows to study the effect of various variables of tethered layers, such as the surface coverage, the attraction between polymers and gels, and the composition of block copolymers. These theoretical results provide guidelines for experimental designs of novel gel materials with tethered layers. © 2001 American Institute of Physics. [DOI: 10.1063/1.1345723]

## I. INTRODUCTION

Hydrogels are of great interest due to their wide range of biomedical applications or their use as model systems for some natural living tissues.<sup>1</sup> Therefore, gel/gel adhesion in an aqueous environment is used to model the interactions between synthetic hydrogels and natural tissues, such as in hydrogel mucoadhesion.<sup>2</sup> It is a primary interest in the biomaterials field to understand and control the interaction between gels.

Another motivation to study gel/gel interactions is the design of self-assembly systems using gel particles. Assemblies of gels of different types possess combination functions of the various components,<sup>3–5</sup> and hence can be used as novel supramolecular materials such as artificial tissues.<sup>6</sup> In this case, it is essential to control the gel/gel interactions such as the equilibrium interparticle distances and the reversibility of the coagulation.

One way to control the gel/gel adhesion is by using tethered polymers on gel surfaces. In the last two decades, tethered chain systems have received considerable attention in colloidal stabilization,<sup>7</sup> protein adsorption prevention,<sup>8,9</sup> and solid/elastomer adhesion.<sup>10</sup> Consequently, the properties and behavior of polymer chains tethered on solid surfaces are relatively well understood.<sup>11–13</sup> On the other hand, polymers tethered on gel surfaces are different from those on solid surfaces since gels are “penetrable” media. Therefore, the bulk structure of gels is also important to understand the behavior of those tethered polymers.

The objective of this work is to theoretically examine the effect of tethered polymers on gel/gel adhesion. The results will provide guidelines for the experimental design of tethered layers on gel surfaces. Recently, a similar system, the elastomer/tethered solid adhesion, has been studied both ex-

perimentally and theoretically.<sup>10,14</sup> Ligoure<sup>14</sup> used a self-consistent mean-field model and studied the adhesion between a polymer brush and elastomer. It was assumed<sup>14,15</sup> that only a fraction of polymers penetrated into the elastomer while others were reflected at the interface between the elastomer and the passive layer. The partition of tethered polymers provided an interfacial energy of entropic origin, which was taken as the driving force for the chain penetration. The penetrated polymers swelled the elastomer and caused an energy penalty. Analytical results were provided on the relations between the adhesion energy and the polymer brush structures.<sup>14</sup>

Our system, which consists of two swollen gels in the aqueous solution, is certainly different. First, we are interested in the case where the tethered polymers are attached to a penetrable medium, a base gel. Second, we want to understand the cases in which the polymer chains are relatively short, up to a hundred segments, and the surface coverages vary from small to large. Thus, we need to apply a molecular approach that enables the study of the polymer chain in a more detailed way and that is applicable in a wider range of surface coverage than the cases studied by Ligoure.<sup>14</sup> While our approach is more detailed in the description of the polymer chains, we describe the gels as environments that do not change upon the penetration of the tethered polymers. This approximation enables us to systematically study the changes in the adhesion between the gels resulting from the changes in the molecular architecture of the tethered polymers.

Our studies are based on the application of a molecular theory that has been successfully used to describe the conformational and thermodynamic properties of tethered polymer layers under many different conditions for short to moderate chain length polymers at all surface coverage.<sup>9,13,16,17</sup> In particular, in recent studies the theory has been shown to provide a quantitative description of the pressure-area isotherms of polystyrene-polyethylene oxide (PS-PEO) spread

<sup>a)</sup> Author to whom correspondence should be addressed.

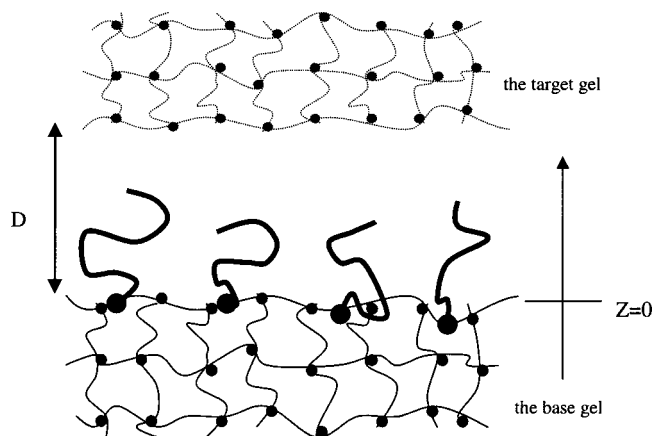


FIG. 1. Schematic representation of the system including the base gel, the target gel, and tethered polymers tethered on the base gel surface. The position  $z=0$  represents the base gel surface plane, and  $z>0$  for the space outside the base gel while  $z<0$  for the space inside the base gel. The distance between two gel surfaces is  $D$ .

at the water/air interface<sup>18</sup> as well as the ability of tethered PEO to prevent protein adsorption.<sup>19,20</sup> The ability of the theory to quantitatively describe experimental systems, as well as to describe the systems at a detailed molecular level, provides us a tool that can be used for the molecular design to achieve optimal gel–gel adhesion.

The article is organized as follows: Sec. II describes the theoretical method we used. Section III shows how the gel/gel interaction can be tailored by using designed tethered structures on gel surfaces. Section IV summarizes the results with some concluding remarks.

## II. THEORETICAL METHOD

In this work, the single-chain mean-field (SCMF) theory<sup>13</sup> is used to study the tethered polymers on gel surfaces. The SCMF theory is based on looking at a polymer chain with all its intramolecular interactions exactly taken into account (within the choice of the appropriate chain model). The intermolecular interactions (including the interaction with other tethered polymers, with solvent molecules, and with gel polymers in the system) are considered within a mean-free approximation. The SCMF theory has been shown especially suitable to study tethered polymers from very short to moderate chain length and at all surface coverage.<sup>13</sup> These are the cases describing most of the biomedical applications.

The theory enables the incorporation of detailed conformational and chemical structure of the polymers through the exact treatment of the chain conformations.<sup>13</sup> This is especially important for experimental designs of desired systems.

The system of interest is composed of two hydrogels (the base gel and the target gel) at equilibrium with their aqueous environment as shown in Fig. 1. Polymer chains are tethered on the base gel surface at a surface coverage,  $\sigma = N_p/A$ , where  $N_p$  is the total number of the tethered chains on the base gel surface and  $A$  is the total surface area of the base gel.

The direction perpendicular to the planar gel surface is indicated as the  $z$ -direction, while the base gel surface corre-

sponds to  $z=0$  plane (see Fig. 1). The system is assumed to be homogeneous in the  $xy$  plane and the only inhomogeneity is in the  $z$  direction.

The tethered polymer chains are modeled as  $n$  connected segments each of volume  $v$  and bond length  $l$ . The volume of solvent molecules is also taken as  $v$  for simplicity. The two hydrogels are modeled as homogeneous and their surfaces are assumed uniform and sharp.  $\phi_b$  and  $\phi_t$  represent the polymer volume fractions of the base gel and target gel, respectively.

The derivation of the theory is based on the minimization of the system's free energy. We separate the interaction potential into repulsive and attractive parts.<sup>13</sup> The repulsive potential is modeled with hard-core excluded volume interactions. The repulsion among the segments within each tethered chain is considered by using self-avoiding tethered chain conformations. The intermolecular repulsive interactions are taken into account in an average way by packing constraints. We define the layer  $z$  as the volume between  $z$  and  $z+dz$ . The packing constraint condition at each layer is described by

$$\langle \phi_p(z) \rangle + \langle \phi_s(z) \rangle + \phi_b(z) + \phi_t(z) = 1, \quad (1)$$

where  $\langle \rangle$  denotes ensemble average,  $\phi$  represent the volume fractions of the components in layer  $z$ , and the subscripts  $p$ ,  $s$ ,  $b$ , and  $t$  denote tethered polymers, solvent molecules, the base gel polymers and the target gel polymers, respectively. This constraint condition means that the volume of layer  $z$  is occupied by the segments from the tethered polymers, the gel polymers and the solvent molecules.

In each layer  $z$ , the volume fraction of tethered polymers is related to the average number of segments per chain  $\langle n(z) \rangle$  in the same layer by

$$\langle \phi_p(z) \rangle = \frac{N_p \langle n(z) \rangle v}{A dz} = \sigma \sum_{\alpha} P_{\alpha} n_{\alpha}(z) v, \quad (2)$$

where  $P_{\alpha}$  is the probability distribution function (pdf) of a chain in conformation  $\alpha$ , and  $n_{\alpha}(z) dz$  is the number of the segments that the tethered chain in conformation  $\alpha$  has at layer  $z$ .

We assume good solvent conditions for polymers. Namely, the tethered polymer–solvent mixture is athermal. We only consider attractive interactions between tethered polymers and gel polymers which is described as the sum of those of the consisting segments. Each segment of polymers is interacting with its environment through an average potential, which depends on the composition of the environment around the segment. Thus, the intermolecular attractions of a tethered chain in conformation  $\alpha$  with the gel polymers is represented by

$$f_1 = kT \int_{-\infty}^{+\infty} n_{\alpha}(z) dz \int_{-\infty}^{+\infty} (\chi_{tp} C(z, z') \phi_t(z') + \chi_{bp} C(z, z') \phi_b(z')) dz'. \quad (3)$$

Here,  $\chi_{tp}$  is the strength of the attraction between the tethered polymer chain segments and the target gel chain segments, while  $\chi_{bp}$  is the strength of the attraction between the tethered polymer chain segments and the base gel. The mag-

nitude of these two nonpositive parameters indicates the extent of the attraction. The van der Waals-type parameters,  $C(z, z')$ , are functions of  $z$ -direction distance  $|z - z'|$  and account for the contribution of a chain segment at layer  $z$  and the gel polymers<sup>13</sup> at layer  $z'$ . Integration over  $z$  and  $z'$  counts all the segments of the specific tethered chain and all the gel polymers in the system, respectively. Note that the interaction between tethered chains and the gel polymers depend on the chain conformation due to the fact that the gel polymer density is inhomogeneous in the  $z$ -direction.

The free energy of the system also has entropic contributions, which includes the conformational and the translational entropy terms. The conformational entropy of tethered chains is of the form

$$S_c = -kN_p \sum_{\{\alpha\}} P_\alpha \ln P_\alpha, \quad (4)$$

where the sum runs over all the possible conformation of the tethered chain, and  $k$  is the Boltzmann constant. The translational entropy of solvent molecules in layer  $z$  is

$$S_t = -kN_s(z) \ln \phi_s(z), \quad (5)$$

where  $N_s(z)$  is the number of solvent molecules at  $z$ .

The free energy per unit interface area is written as the sum of the above terms, and take the following form:

$$\begin{aligned} \frac{F}{AkT} = & \sigma \left\{ \sum_{\{\alpha\}} P_\alpha \ln(P_\alpha) + \int_{-\infty}^{+\infty} \sum_{\{\alpha\}} P_\alpha n_\alpha(z) \right. \\ & \times \int_{-\infty}^{+\infty} [\chi_{tp} C(z, z') \phi_t(z') \\ & + \chi_{bp} C(z, z') \phi_b(z')] dz dz' \left. \right\} \\ & + \int_{-\infty}^{+\infty} \phi_s(z) \ln(\phi_s(z)) v^{-1} dz, \end{aligned} \quad (6)$$

where  $F$  is the free energy of the whole system.

The free energy is a function of the pdf of the tethered chain conformation  $P_\alpha$  and the solvent density profile in different layers,  $\phi_s(z)$ . These two quantities are determined by minimization of the free energy expression of Eq. (6) subject to the packing constraint of Eq. (1). Introducing Lagrange multipliers  $\pi(z)$  the minimization procedure yields

$$\begin{aligned} P_\alpha = & \frac{1}{q} \exp \left\{ - \int_{-\infty}^{+\infty} n_\alpha(z) dz \int_{-\infty}^{+\infty} [\chi_{bp} C(z, z') \phi_b(z') \right. \\ & + \chi_{tp} C(z, z') \phi_t(z')] dz' \left. \right\} \\ & \times \exp \left\{ - \int_{-\infty}^{+\infty} \pi(z) n_\alpha(z) v dz \right\}, \end{aligned} \quad (7)$$

$$\phi_s(z) = \exp \{ - \pi(z) v \}, \quad (8)$$

where  $q$  is the normalized factor for the pdf.

The only unknowns to determine the pdf and solvent density profiles are the  $\pi(z)$ . After introducing Eqs. (7) and (8) back into the packing constraint condition, Eq. (1), a set

of equations for the unknown  $\pi(z)$  is obtained. We solve them as functions of the surface coverage  $\sigma$ , the volume fraction of two gels  $\phi_b$  and  $\phi_t$ , and the attraction parameters between tethered chain segments and gel polymers  $\chi_{tp}$  and  $\chi_{bp}$ .

To implement the calculation, we discretize the space into layers of finite thickness  $\delta$ . It has been shown<sup>13</sup> that the results of the calculations are independent of the choice of  $\delta$  provided its value is between  $1.0 l$  and  $2.0 l$ , where  $l$  is the tethered polymer bond length. In this work, we take  $\delta$  as  $1.86 l$  for computational convenience, and solve a finite set of coupled nonlinear equations for the discretized  $\pi(z)$  by using standard numerical methods. The form of  $C(z, z')$  in Eq. (3) is obtained by integrating the average attractive interactions over the whole volume of each different layer (as indicated in detail before<sup>13</sup>). Throughout this work, an attraction parameter  $\chi = -1$  corresponds to a segment pair potential of van der Waals-type with the depth minimum  $\epsilon = kT$ . Upon solution of the set of equations for  $\pi(z)$  we can calculate the chain conformation pdf  $P_\alpha$  using Eq. (7); then all the average properties of the system can be obtained.

The chain model used for the chain conformation is the rotational isomeric state (RIS) model with self-avoiding interactions. Specifically, each bond has three possible states (*trans*, *gauche*<sup>+</sup>, and *gauche*<sup>-</sup>), and we take the three states to have the same internal energy, that is, the tethered chains are fully flexible. For all the calculations in this work, a set of  $10^6$  different chain conformations is used for each kind of tethered chains. It was tested that further increasing the number of conformations in the set does not change the results.

The above equations, though explicitly written for the homopolymer tethered chains, can be used for block copolymers by recognizing that the segments in different blocks have different interactions with the two gels. The derivation of the chain conformation pdf is based on the same process to obtain Eq. (7), while Eq. (3) is modified to include the different attraction parameters between gels and the different blocks. The tethered diblock copolymers with blocks  $A$  and  $B$  have their conformation pdf of the following form:

$$\begin{aligned} P_\alpha = & q^{-1} \exp \left\{ - \int_{-\infty}^{+\infty} n_{\alpha A}(z) dz \int_{-\infty}^{+\infty} [\chi_{bpA} C(z, z') \phi_b(z') \right. \\ & + \chi_{tpA} C(z, z') \phi_t(z')] dz' \left. \right\} \exp \left\{ - \int_{-\infty}^{+\infty} n_{\alpha B}(z) dz \right. \\ & \times \int_{-\infty}^{+\infty} [\chi_{bpB} C(z, z') \phi_b(z') + \chi_{tpB} C(z, z') \phi_t(z')] dz' \left. \right\} \\ & \times \exp \left\{ - \int_{-\infty}^{+\infty} \pi(z) (n_{\alpha A}(z) + n_{\alpha B}(z)) v dz \right\}. \end{aligned} \quad (9)$$

Here parameters  $n_{\alpha A}(z) dz$  and  $n_{\alpha B}(z) dz$  are the number of segments of block  $A$  and  $B$ , respectively in the conformation  $\alpha$  that are in layer  $z$ . In deriving Eq. (9) it was assumed that the two segments of the two blocks have the same volume.

### III. RESULTS AND DISCUSSION

In this section, we used the theory to investigate the effect of the tethered layer on the gel/gel interactions. The

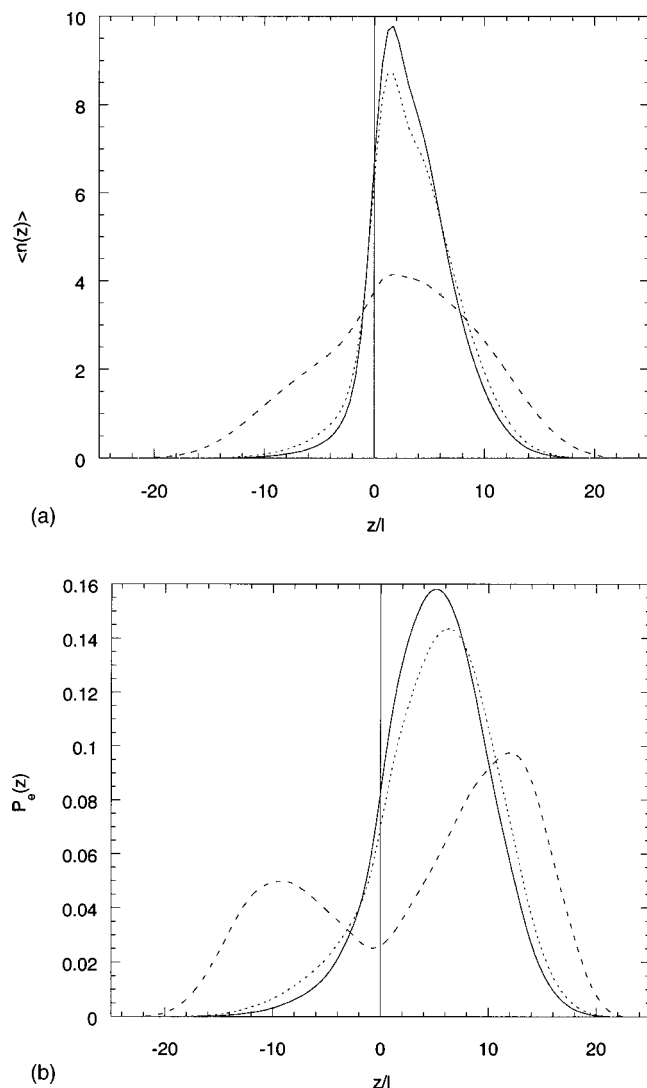


FIG. 2. (a) The average number of segments per tethered polymer as a function of the distance from the tethered surface for three different surface coverages. The surface coverages,  $\sigma l^2$  are 0.001 (solid line), 0.01 (dotted line), and 0.1 (dashed line), respectively.  $l$  is the segment length of tethered polymers. Other physical parameters include:  $\phi_b = 0.1$ , tethered polymer length  $n = 40$ , all of the interaction parameters are zero. (b) The probability of finding the free end segment of tethered polymers as a function of the distance from the tethered surface for the same three cases in (a).

structure of the tethered layer determines the polymer behavior in the gel/gel adhesion. Compared with the structure on the solid substrates, the structure of the tethered layer on a gel surface depends on the gel properties such as the volume fraction of the gel and the interaction between gel polymers and tethered chains. Figure 2(a) shows the average number of the polymer segments as a function of the distance from the base gel surface for 40-segment tethered chains on a base gel with  $\phi_b = 0.1$  and with different surface coverages  $\sigma$ . Throughout this work, we fix the polymer volume fraction of the target gel  $\phi_t = 0.1$  (which is a good model for the human mucus<sup>2</sup>), and vary the other parameters.

As mentioned before, the tethered polymers can penetrate into the base gel as well as stretch out of it. It is shown in Fig. 2(a) that the segments distribute asymmetrically across the tethered surface due to the repulsion between teth-

ered polymers and the base gel polymers. The segment distribution depends on the surface coverage as well as the base gel properties. In the low surface coverage cases, most of the segments are outside of the base gel, because the dominant interaction is the repulsion between the tethered polymer and the base gel. Increasing surface coverage, the asymmetry extent becomes less significant due to the increasing repulsion among tethered polymers in the outside layer. Namely, the structure of the tethered polymer layer is the result of the optimal molecular structure that can be achieved considering the repulsion between the tethered chains among themselves and with the base gel.

The free chain end distribution is important for the kinetics of chain interpenetration in gel/gel adhesion.<sup>21</sup> Figure 2(b) shows the distribution of the free end segments of the tethered chains as a function of the distance from the base gel surfaces for the same cases shown in Fig. 2(a). At low surface coverage most of the free end segments are outside the base gel, which is consistent with the segment distributions in Fig. 2(a). As the surface coverage increases, for the layer outside the base gel, the maximum of the distribution shifts further from the surface; on the other hand, the fraction of tethered chains with end segments inside the gel also increases. An interesting result is that at some relatively high surface coverage the chain ends have a bimodal distribution. Those tethered chains with their ends inside the base gel will be expected to have slower kinetics when penetrating into the approaching gel, because they need to move out of the base gel before penetrating into the target gel.

Increasing the volume fraction of the base gel shifts more tethered polymer segments outside of the gel, provided that there is no attraction between them. The extreme case is for the gel with  $\phi_b = 1$ , that is, a solid substrate. However, if the attraction between tethered polymers and gel polymers is strong enough, most of the polymer segments situate inside the gel, and leave a very thin tethered layer outside, which hence has little effect on the gel/gel interaction.

In this work, we assume that there is no attraction between the two bare surfaces of the gels in order to study the effect of the tethered layer. To characterize the effect of tethered polymers on gel/gel adhesion, we define the dimensionless free energy change of the system,  $F/kT$ , divide by the number of tethered polymers  $N_p$ , as  $f$ ,

$$f = \frac{F}{N_p kT} = \frac{F}{A \sigma kT}. \quad (10)$$

This parameter  $f$  represents the contributions per tethered chain to the interaction between the base gel and the target gel. We calculate  $f$  as a function of the gel/gel interface distance,  $D$ , for different tethered structures. Practically, the free energy per unit interface area,  $F/A$ , as a function of interface distance  $D$  can be measured by using the surface force apparatus.<sup>22</sup> The following theoretical prediction of  $f$  vs  $D/l$  curves can be transformed to compare with the measurable  $F/A$  vs  $D$  data after definition of the basic chain parameter  $l$ . If  $f$  decreases with decreasing  $D$ , i.e., if the two gels get contact spontaneously in the aqueous environment, we conclude that tethered polymers enhance the gel/gel adhesion.



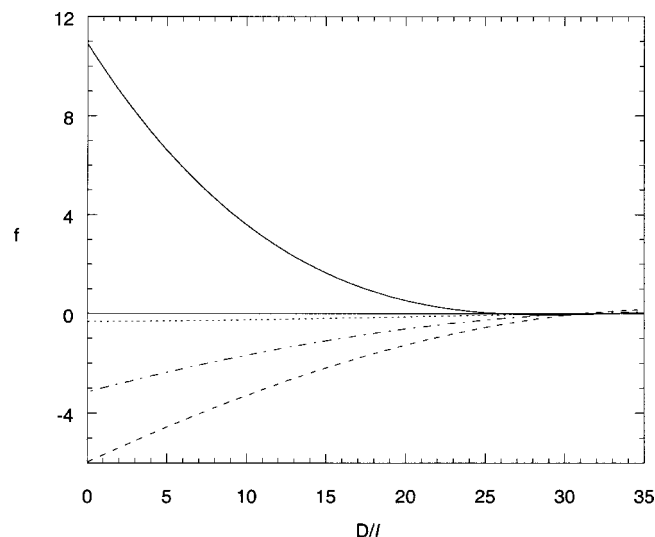


FIG. 3. The free energy per tethered polymer,  $f$ , as a function of  $D$  for four different  $\chi_{tp}$  cases:  $\chi_{tp}=0.0$  (solid line),  $-0.2$  (dotted line),  $-0.25$  (dotted-dashed line), and  $-0.3$  (dashed line). In all cases  $\phi_b=0.3$ , tethered polymer length  $n=100$ , all of the other interaction parameters are zero.

Otherwise, tethered layers provide a repulsion barrier for gels as expected in the normal colloidal stabilization cases.

Figure 3 shows  $f$  as a function of the gel/gel distance for the same gels with four different values of interaction parameters between tethered polymers and the target gel polymers. When there is no attraction between the two polymers, the tethered layer introduces an extra repulsion barrier for two gels. It is noteworthy that the free energy penalty for complete contact of two gels is smaller than if the polymers were tethered on solid substrates. This is due to the fact that the base gel provides extra space for tethered polymers to rearrange themselves. By choosing the chemical structure of tethered polymers and hence increasing their attraction with the target gel polymers, the gel/gel adhesion becomes thermodynamically favorable and tethered chains contribute to the adhesion strength, which is shown in the other three curves in Fig. 3. The contribution to the adhesion energy from each chain is defined by the negative free energy change,  $f_0$  at  $D=0$ , and the dimensionless adhesion energy per unit interface area is  $W=F_0/AkT=f_0\sigma$ .

The interaction between the tethered layer and the approaching target gel changes the molecular organization of polymers, which can be shown by the changes of segment distribution profiles of tethered polymers with the change of interface distance. In the case without polymer/gel attraction, the tethered polymers are compressed inside the gap when the two gels try to get closer to each other. In the case with attraction between tethered polymers and the target gel, the polymer chains spontaneously penetrate into the target gel in the favorable gel/gel contact process.

The average contribution per tethered chain to the adhesion is a function not only of the chain length and the polymer/gel attraction parameter, but also of the surface coverage of the tethered layer. Figure 4(a) shows the free energy profiles of three different cases. The contribution per chain to the adhesion energy decreases as the surface coverage increases provided other parameters are the same. Figure 4(b)

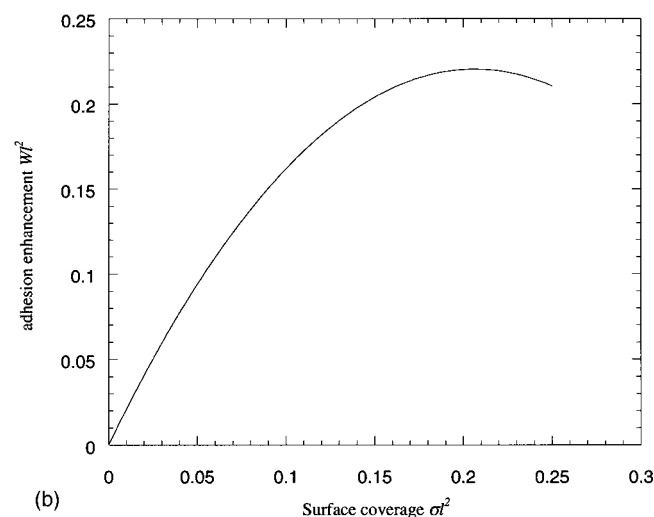
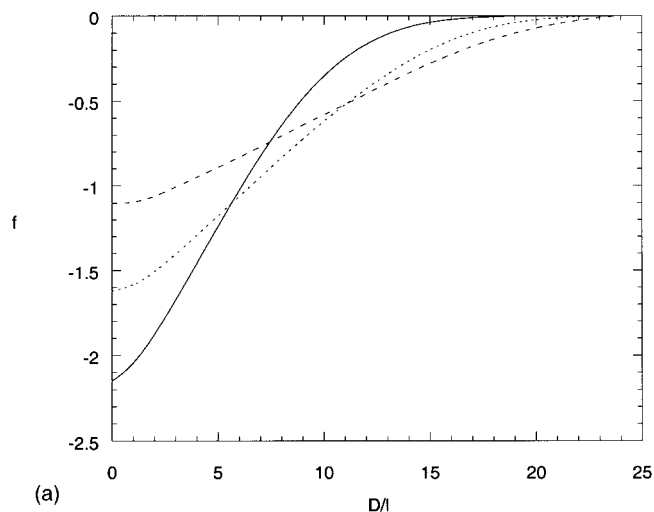


FIG. 4. (a) The free energy of the system per tethered polymer,  $f$ , as a function of  $D$  for different cases of the surface coverage:  $\sigma l^2=0.01$  (solid line),  $0.1$  (dotted line), and  $0.2$  (dashed line). In all cases  $\phi_b=0.3$ , tethered polymer length  $n=40$ ,  $\chi_{tp}=-0.3$ , and  $\chi_{bp}=0.0$ . (b) The adhesion energy as a function of surface coverages for the cases shown in (a).

shows the dimensionless adhesion energy,  $Wl^2$ , as a function of surface coverage of tethered polymers. Clearly a maximum adhesion is achieved under some optimal tethered structures. This is similar to the experimental observation in the elastomer/tethered solid systems.<sup>10</sup>

Based on the above discussion, the qualitative interaction between two gels can be altered by the choice of tethered polymers, especially the attraction parameter between tethered polymers and gel polymers. However, the detailed gel/gel interface structure and interactions are also important for optimized performance, such as in the case of the self-assembly of gel particles. In the following, we will show that the use of block copolymers in the tethered layer can lead to tuning of the gel/gel interactions.

The block copolymers consist of two types of blocks, A and B, where the block A is the anchoring block. Figure 5 shows how the equilibrium gel/gel distances can be controlled by using these diblock copolymers with different compositions. The equilibrium distances of different systems

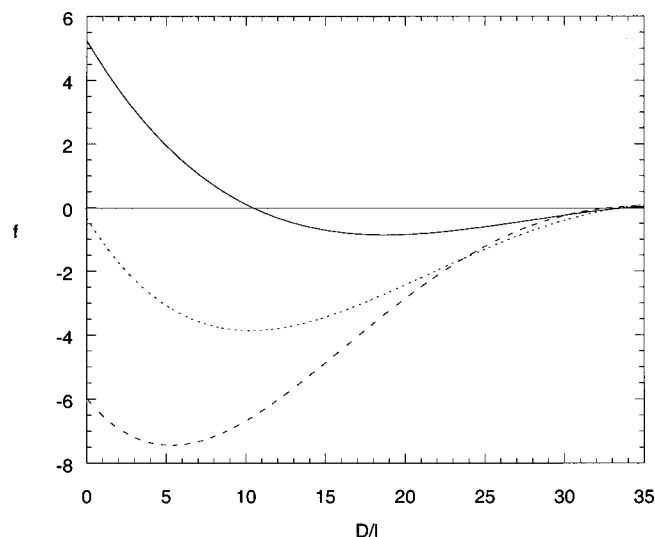


FIG. 5. The free energy per tethered polymer,  $f$ , as a function of  $D$  for cases of diblock  $AB$  copolymers with different compositions:  $A+B=75+25$  (solid line),  $50+50$  (dotted line), and  $25+75$  (dashed line). Other physical variables include:  $\phi_b=0.3$ ,  $\sigma l^2=0.01$ ,  $\chi_{tpA}=0.0$ ,  $\chi_{tpB}=-0.4$ , and  $\chi_{bpA}=\chi_{bpB}=0.0$ .

are indicated by the minimum in the free energy profile curves. In these diblock copolymers, the first block (block A) is repulsive to the target gel, while monomers in the block B are attractive to it. Initially the outer layer of the tethered structure mainly consists of the segments of the block B, and provide attraction for the target gel. The penetration process will continue until reaching some intermediate interface distance, where the attraction between the target gel and the block B is compromised by the repulsion by the block A. Note that the use of homopolymers of the same two monomers would cause either pure repulsion or complete contact between gels.

Figure 6 shows the segment distributions of the two blocks under the equilibrium interface distance for one of the copolymer tethered layers shown in Fig. 5. The two gel surfaces are indicated by the two vertical lines, while the data of block A and B are represented by the solid and dotted lines, respectively. It is shown that the first block mainly resides in the gap between two gels, while the second block penetrates into the target gel. In this case, the tethered layer brings the two gels together without letting them completely contact.

The adhesion fracture strength between two gels with tethered layers is expected to depend on the detailed structure of these connector polymers.<sup>23,24</sup> The tethered chains have one end covalently bound on the surface of one gel, but they can penetrate into both sides and form various bridge structures across the interface, such as the so-called “many-stitch” structure.<sup>24</sup> In the following we will show that the use of copolymers as tethered chains is able to specifically design the bridge structures.

Figure 7 shows the segment distribution profiles of the two blocks of tethered copolymers across the gel/gel interface, i.e., at distance  $D=0$  between the two gels. In the figure, the target gel is in the positive- $z$  side while the base gel is in the negative- $z$  side. We see that the first block, which originates from the tethering segment, mainly distrib-

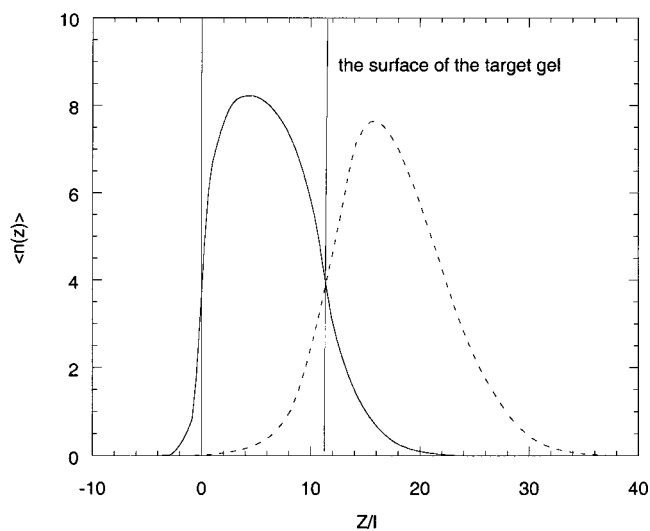


FIG. 6. The average number of segments of each block in copolymer  $AB$  as a function of the distance from the tethered surface: block A (solid line) and block B (dashed line). The copolymer is  $A+B=50+50$ , and the distance between two gels is the equilibrium distance shown in Fig. 5. All the other parameters are the same as in Fig. 5. The vertical line at  $z/l=11$  represents the surface plane of the target gel. Therefore, the segments with  $z<0$  are within the base gel, those with  $z>0$  but behind the vertical dotted line are in the gap between two gels, and those beyond the vertical line are within the target gel.

utes inside the target gel, however, the remaining part of the tethered polymer has significant fraction of segments inside the base gel. The more detailed segment distribution data suggest the most probable chain conformation is as shown in Fig. 8; the tethered chains first penetrate into the target gel, and then come back to the base gel, i.e., forming a looplike interface conformation.

The looplike conformation distribution can be tuned by changing the composition of the tethered copolymers. Taking a 40-segment diblock chain as an example, we quantita-

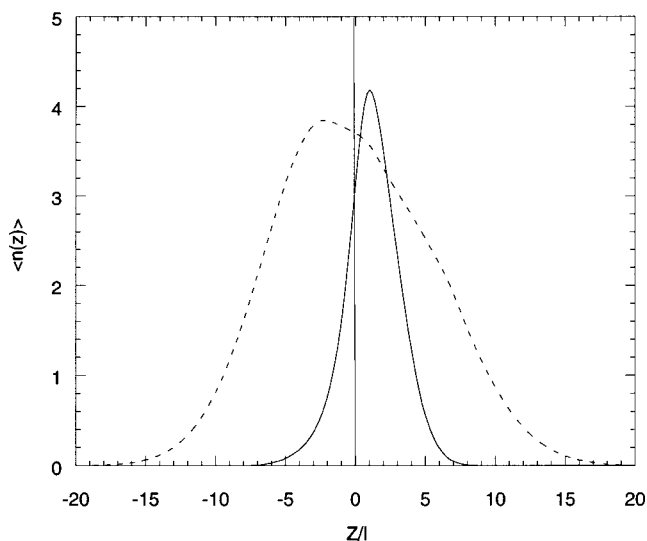


FIG. 7. The average number of segments of each block in copolymer  $AB$  as a function of the distance from the tethered surface: block A (solid line) and block B (dashed line). The copolymer is  $A+B=10+30$ , and the distance between two gels is zero. In all cases  $\phi_b=0.3$ ,  $\sigma l^2=0.01$ ,  $\chi_{tpA}=\chi_{tpB}=-0.3$ , and  $\chi_{bpA}=0$ ,  $\chi_{bpB}=-0.3$ .

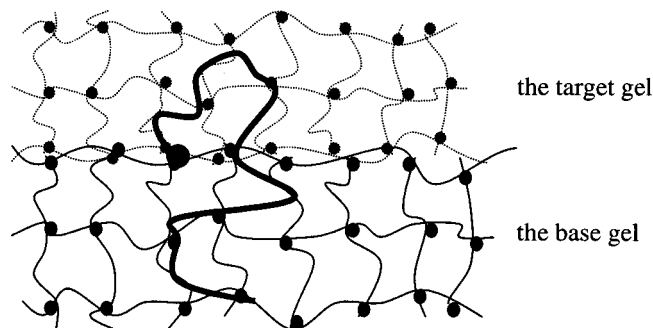


FIG. 8. The schematic representation of the most probable conformation of the tethered copolymers at the gel/gel interface under the conditions specified in Fig. 7. The polymers, which tethered on the base gel surface, first penetrate into the target gel side, and then go back into the base gel side.

tively define the looplike conformation as the following: the tenth segment situates in the target gel with a penetration depth larger than  $\delta$ , which is about 5.5 Å for poly(ethylene glycol) (PEG), and the fortieth segment is inside the base gel also with a penetration depth beyond  $\delta$ . Figure 9 shows the probability of this looplike conformation that the tethered copolymers take as a function of the fraction of the second block, block *B*, in the copolymers. It is shown that this probability reaches a maximum at some intermediate composition of the copolymers.

#### IV. CONCLUDING REMARKS

We have studied the effect of tethered polymers on the gel/gel adhesion by using the single-chain mean-field theory. We have shown that the gel surface structure, the gel/gel adhesion strength, the equilibrium gel/gel distance, and the detailed interface structure can be tailored by specifically designing tethered layers on gel surfaces.

The bulk properties of the gel, on whose surface the polymers are tethered, have an important effect on the tethered structure. Depending on the volume fraction of the gel

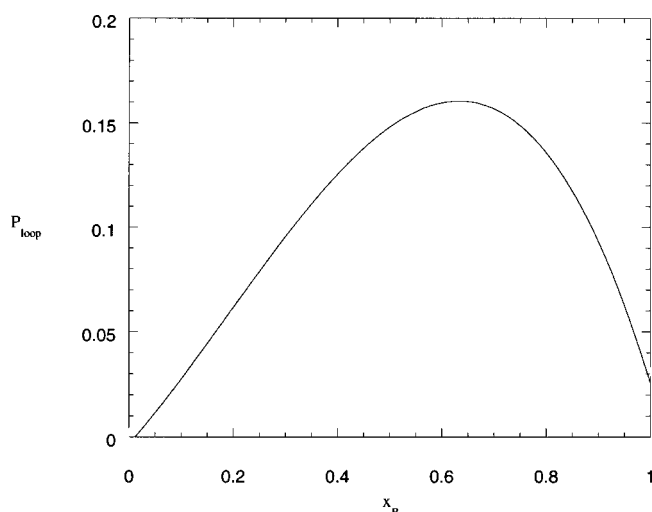


FIG. 9. The probability of tethered chains in looplike conformation as a function of the fraction of the *B* block in the copolymers. The copolymer has 40 segments, and the distance between the two gels is zero. In all cases  $\phi_b = 0.3$ ,  $\sigma l^2 = 0.01$ ,  $\chi_{tPA} = \chi_{tPB} = -0.3$ , and  $\chi_{bPA} = 0$ ,  $\chi_{bPB} = -0.3$ .

and the interaction between gel and polymers, the tethered chains exhibit different partition across the interface between gel and the aqueous environment, which in turn affects the initial interaction between two gels. By tethering different polymers on the base gel surface, the interaction between gels can be modified from pure repulsion to spontaneous adhesion. In the adhesion process, the tethered chains penetrate into the coming gel and form bridges between the two gels.

The use of block copolymers at the gel surface provides more detailed control on the gel/gel interaction. The interface distance, where is an attractive minimum, can be tuned by using copolymers with different compositions. This suggests the use of tethered copolymers to design the self-assembly systems of gels. The conformation of these copolymers across the gel/gel interface may also be tuned, such as the formation of the looplike structures.

We used a simple model for the gels for which we assume that they are in the equilibrium swollen state and their properties are not changed by the chain penetration. This limits our ability to include the specific parameters of gels such as the mesh chain lengths. In some cases, the existence of free polymers in a swollen gel may cause gel collapse. For example, the addition of PEG chains resulted in the collapse of poly(methacrylic acid) gels due to the complex formation between gels and the linear polymer.<sup>25</sup> Obviously, a more descriptive model of swollen gels will be used in further studies.

The theoretical predications may be tested by direct force measurement techniques, for example, by using the surface force apparatus. It should be emphasized that the results shown here are the equilibrium data, and that the calculated adhesion enhancement corresponds to the case of zero separation rate.<sup>23,24</sup> The dynamic aspect of the adhesion test with connected chains at the interface is rather complicated. Recent experimental<sup>26,27</sup> and theoretical studies<sup>23,24,28–32</sup> as well as computer simulations<sup>33,34</sup> have been discussed in the literature.

#### ACKNOWLEDGMENTS

This work is supported in part by National Institute of Health through Grant No. GM56321 and National Science Foundation Grant No. BES-9706538. I.S. is a Camille Dreyfus Teacher-Scholar and he acknowledges partial support from National Science Foundation.

<sup>1</sup>N. A. Peppas, *Hydrogels in Medicine and Pharmacy* (CRC Press, Boca Raton, 1986).

<sup>2</sup>A. G. Mikos and N. A. Peppas, in *Bioadhesive Drug Delivery Systems*, edited by V. Lenaerts and R. Gurny (CRC Press, Boca Raton, 1986).

<sup>3</sup>O. D. Velev, K. Furusawa, and K. Nagayama, *Langmuir* **12**, 2374 (1996).

<sup>4</sup>Z. Hu, X. Lu, J. Gao, and C. Wang, *Adv. Mater.* **12**, 1173 (2000).

<sup>5</sup>T. Serizawa, K. Taniguchi, and M. Akashi, *Colloids Surf., A* **169**, 95 (2000).

<sup>6</sup>S. Chiruvolu, S. Walker, J. Israelachvili, F. Schmitt, D. Leckband, and J. A. Zasadzinski, *Science* **264**, 1753 (1994).

<sup>7</sup>D. H. Napper, *Polymeric Stabilization of Colloidal Dispersions* (Academic, New York, 1983).

<sup>8</sup>J. D. Andrade and V. Hlady, *Adv. Polym. Sci.* **79**, 1 (1986).

<sup>9</sup>I. Szleifer, *Curr. Opin. Solid State Mater. Sci.* **2**, 337 (1997).

<sup>10</sup>L. Leger, E. Raphael, and H. Hervet, *Adv. Polym. Sci.* **138**, 185 (1999).

<sup>11</sup>S. T. Milner, *Science* **251**, 905 (1991).

- <sup>12</sup>A. Halperin, M. Tirrell, and T. P. Lodge, *Adv. Polym. Sci.* **100**, 31 (1992).
- <sup>13</sup>I. Szleifer and M. A. Carignano, *Adv. Chem. Phys.* **94**, 165 (1996).
- <sup>14</sup>C. Ligoure, *Macromolecules* **29**, 5459 (1996).
- <sup>15</sup>F. Brochard-Wyart, P. G. de Gennes, L. Léger, Y. Marciano, and E. Raphaël, *J. Phys. Chem.* **98**, 9405 (1994).
- <sup>16</sup>I. Szleifer, *Curr. Opin. Colloid Interface Sci.* **1**, 416 (1996).
- <sup>17</sup>I. Szleifer and M. A. Carignano, *Macromol. Rapid Commun.* **21**, 423 (2000).
- <sup>18</sup>M. C. Fauré, P. Bassereau, M. A. Carignano, I. Szleifer, Y. Gallot, and D. Andelman, *Eur. Phys. J. B* **3**, 365 (1998).
- <sup>19</sup>T. McPherson, A. Kidane, I. Szleifer, and K. Park, *Langmuir* **14**, 176 (1998).
- <sup>20</sup>J. Satulovsky, M. A. Carignano, and I. Szleifer, *Proc. Natl. Acad. Sci. U.S.A.* **97**, 9037 (2000).
- <sup>21</sup>K. P. O'Connor and T. C. B. McLeish, *Macromolecules* **26**, 7322 (1993).
- <sup>22</sup>J. Israelachvili, *Intermolecular and Surface Forces* (Academic, San Diego, 1991).
- <sup>23</sup>E. Raphaël and P. G. de Gennes, *J. Phys. Chem.* **96**, 4002 (1992).
- <sup>24</sup>H. Ji and P. G. de Gennes, *Macromolecules* **26**, 520 (1993).
- <sup>25</sup>O. E. Philippova, N. S. Karibyants, and S. G. Starodubtzev, *Macromolecules* **27**, 2398 (1994).
- <sup>26</sup>H. R. Brown, *Macromolecules* **26**, 1666 (1993).
- <sup>27</sup>C. Creton, H. Brown, and K. R. Shull, *Macromolecules* **27**, 3174 (1994).
- <sup>28</sup>P. G. de Gennes, *J. Phys. (Paris)* **50**, 2551 (1989).
- <sup>29</sup>K. P. O'Connor and T. C. B. McLeish, *Polymer* **33**, 4314 (1992).
- <sup>30</sup>B. Lin and P. L. Taylor, *Macromolecules* **27**, 4212 (1994).
- <sup>31</sup>T. N. Krupenkin and P. L. Taylor, *Macromolecules* **28**, 5819 (1995).
- <sup>32</sup>L. Kogan, C.-Y. Hui, and A. Ruina, *Macromolecules* **29**, 4090 (1996); **29**, 4101 (1996).
- <sup>33</sup>J. M. Deutsch and H. Yoon, *J. Chem. Phys.* **102**, 7251 (1995).
- <sup>34</sup>G. T. Pickett, D. Jasnow, and A. C. Balazs, *Phys. Rev. Lett.* **77**, 671 (1996).